Allosteric activation of MALT1 by its ubiquitin-binding Ig3 domain

Rebekka Schairer[a,1], Gareth Hall[b,c,1], Ming Zhang[a,1,2], Richard Cowan[b,c], Roberta Baravalle[b,c], Frederick W. Muskett[b,c], Peter J. Coombs[d], Chido Mpamhanga[d], Lisa R. Hale[d], Barbara Saxty[d], Justyna Iwaszkiewicz[e], Chantal Décaillet[a], Mai Perroud[a], Mark D. Carr[b,c,3], and Margot Thome[a,3]

[a]Department of Biochemistry, University of Lausanne, 1066 Epalinges, Switzerland; [b]Department of Molecular and Cell Biology, University of Leicester, LE1 7RH Leicester, United Kingdom; [c]Leicester Institute of Structural and Chemical Biology, University of Leicester, LE1 7RH Leicester, United Kingdom; [d]LifeArc, Accelerator Building, Open Innovation Campus, SG1 2FX Stevenage, United Kingdom; and [e]Swiss Institute of Bioinformatics, 1015 Lausanne, Switzerland

Edited by Tak W. Mak, University Health Network, Toronto, Canada, and approved December 30, 2019 (received for review July 23, 2019)

The catalytic activity of the protease MALT1 is required for adaptive immune responses and regulatory T (Treg)-cell development, while dysregulated MALT1 activity can lead to lymphoma. MALT1 activation requires its monoubiquitination on lysine 644 (K644) within the Ig3 domain, localized adjacent to the protease domain. The molecular requirements for MALT1 monoubiquitination and the mechanism by which monoubiquitination activates MALT1 had remained elusive. Here, we show that the Ig3 domain interacts directly with ubiquitin and that an intact Ig3-ubiquitin interaction surface is required for the conjugation of ubiquitin to K644. Moreover, by generating constitutively active MALT1 mutants that overcome the need for monoubiquitination, we reveal an allosteric communication between the ubiquitination site K644, the Ig3-protease interaction surface, and the active site of the protease domain. Finally, we show that MALT1 mutants that alter the Ig3-ubiquitin interface impact the biological response of T cells. Thus, ubiquitin binding by the Ig3 domain promotes MALT1 activation by an allosteric mechanism that is essential for its biological function.

protease | structure | ubiquitin | signaling | T cell

The paracaspase MALT1 is a proteolytic enzyme whose function is essential for adaptive immune responses and the development of particular lymphocyte subsets, such as Treg cells, marginal zone, and B1 B cells (1–6). MALT1 is activated upon triggering of the B- or T cell antigen receptors and other immunoreceptors, such as activating natural killer cell (NK) receptors or Fc receptors (7). A variety of G protein coupled receptors and certain tyrosine receptor kinases have also been reported to signal via MALT1 (7). A common feature of MALT1-activating receptors is their capacity to induce the formation of so-called CARMA-BCL10-MALT1 (CBM) complexes, comprising a CARD-containing scaffold protein, the adaptor protein BCL10, and MALT1 (8).

Based on structural studies on in vitro reconstituted CBM signalosomes from lymphocytes, which contain the scaffold protein CARMA1 (also known as CARD11), it has been proposed that the CBM complex adopts a helical filamentous structure in which CARMA1 nucleates the polymerization of BCL10 into filaments that can incorporate MALT1 (9, 10). MALT1 contains an N-terminal death domain (DD) that binds to the core of the BCL10 filament by interacting with the BCL10 CARD motif (9). The MALT1 DD is followed by two Ig-like domains, the protease domain, a third Ig-like domain, and an unstructured C-terminal extension (11, 12). The C-terminal part of MALT1 that comprises the protease domain is thought to protrude from the filamentous core (9), but the exact conformation and activation status of MALT1 within the BCL10/MALT1 fibers remain unknown. The crystallographic analysis of highly purified constructs of MALT1 containing the protease and the adjacent Ig3 domain has revealed that the protease domain can dimerize (13, 14). The dimer crystals additionally show that the protease and Ig3 domains physically interact and undergo a rotational movement upon binding of a substrate analog (13, 14).

Using biochemical approaches, we have previously shown that MALT1 activation requires its monoubiquitination on K644, a lysine residue situated at the surface of the Ig3 domain (15). Moreover, we demonstrated an interaction of ubiquitin with an unknown binding site within the C-terminal half of MALT1, which comprises the protease domain, the Ig3 domain, and a nonstructured C-terminal extension (15). However, the precise location of the ubiquitin-binding site and the way by which ubiquitin binding contributes to MALT1 activation have remained unknown.

Here, we present experimental evidence that suggests that ubiquitin binding to the Ig3 domain is required for MALT1 monoubiquitination, which, in turn, perturbs an inhibitory interaction of the Ig3 domain with the protease domain and induces conformational changes within the catalytic domain that lead to enhanced activity.

Results

Monomeric Ubiquitin Binds to the Ig3 Domain of MALT1. We had previously shown that ubiquitin can interact physically with a C-terminal portion of MALT1 that comprises its protease domain, the Ig3 domain, and a nonstructured C-terminal extension (15).

Significance

The protease MALT1 has been shown to play an essential role in the adaptive immune response and the development of lymphoma. The catalytic activity of MALT1 is tightly regulated by monoubiquitination, however, how ubiquitin is conjugated to MALT1 and the manner by which this modification regulates MALT1 activity remains poorly understood. Our data suggest that the Ig3 domain of MALT1 physically recruits ubiquitin to enable monoubiquitination and that ubiquitin conjugation to MALT1 activates the protease by inducing conformational changes in the Ig3 domain that are communicated to the active site. These findings identify the Ig3 domain of MALT1 as a novel ubiquitin-binding domain and provide insight into the molecular requirements for MALT1 activation that could be of therapeutic interest.

Author contributions: R.S., G.H., M.Z., R.C., R.B., F.W.M., P.J.C., C.M., L.R.H., B.S., M.D.C., and M.T. designed research; R.S., G.H., M.Z., C.D., and M.P. performed research; R.S., G.H., M.Z., R.C., R.B., F.W.M., P.J.C., C.M., L.R.H., B.S., J.I., M.D.C., and M.T. analyzed data; and R.S., G.H., M.D.C., and M.T. wrote the paper.

The authors declare no competing interest.

This article is a PNAS Direct Submission.

[1]R.S., G.H., and M.Z. contributed equally to this work.

[2]Present address: Division of Systems Biology and Personalised Medicine, The Walter and Eliza Hall Institute of Medical Research, 3052 Parkville, Melbourne, VIC, Australia.

[3]To whom correspondence may be addressed. Email: mdc12@leicester.ac.uk or Margot.ThomeMiazza@unil.ch.

This article contains supporting information online at https://www.pnas.org/lookup/suppl/doi:10.1073/pnas.1912681117/-/DCSupplemental.

First published January 24, 2020.

To identify key ubiquitin residues involved in the binding to MALT1, we monitored differences in the $^{15}N/^{1}H$ HSQC spectrum of uniformly labeled ubiquitin (1–76) induced by the addition of MALT1 (Fig. 1*A*). The observed minimal shifts in backbone amide signals of ubiquitin upon MALT1 addition clearly identified a contiguous interaction surface showing significant shifts for 10 residues, including I13, G47, K6, K48, H68, Q49, L69, V70, L71, and R72, centered around I44 (Fig. 1*A* and *SI Appendix*, Fig. S1*A*). These residues are predominantly localized to the β3–β5 strands collectively forming a continuous patch of ∼172 Å^2 on the surface of ubiquitin (Fig. 1*B*). This surface patch comprises several positively charged amino acids, including K6, K48, H68, and R72, which together form a striking positively charged region on ubiquitin (Fig. 1*C*). To identify the MALT1 residues involved in the interaction with ubiquitin, we then generated a soluble monomeric MALT1 construct comprising the protease and Ig3 domain (residues 339–719) and monitored changes in the $^{15}N/^{1}H$ TROSY spectrum of uniformly labeled MALT1 induced by the addition of ubiquitin. Upon addition of increasing concentrations of free ubiquitin, we observed significant shifts in the backbone amide signals of several residues of MALT1, including E624, I625, Y692, L695, E696, D697, and T698 (Fig. 1*D* and *SI Appendix*, Fig. S1*B*). These residues are mainly located within the β3/β4 and β6/β7 loops at the surface of the MALT1 Ig3 domain on the side opposing the Ig3-protease domain interaction surface (Fig. 1*E*), which combine to form a negatively charged area of ∼246 Å^2 on the surface of MALT1 (Fig. 1*F*). To provide additional evidence for the

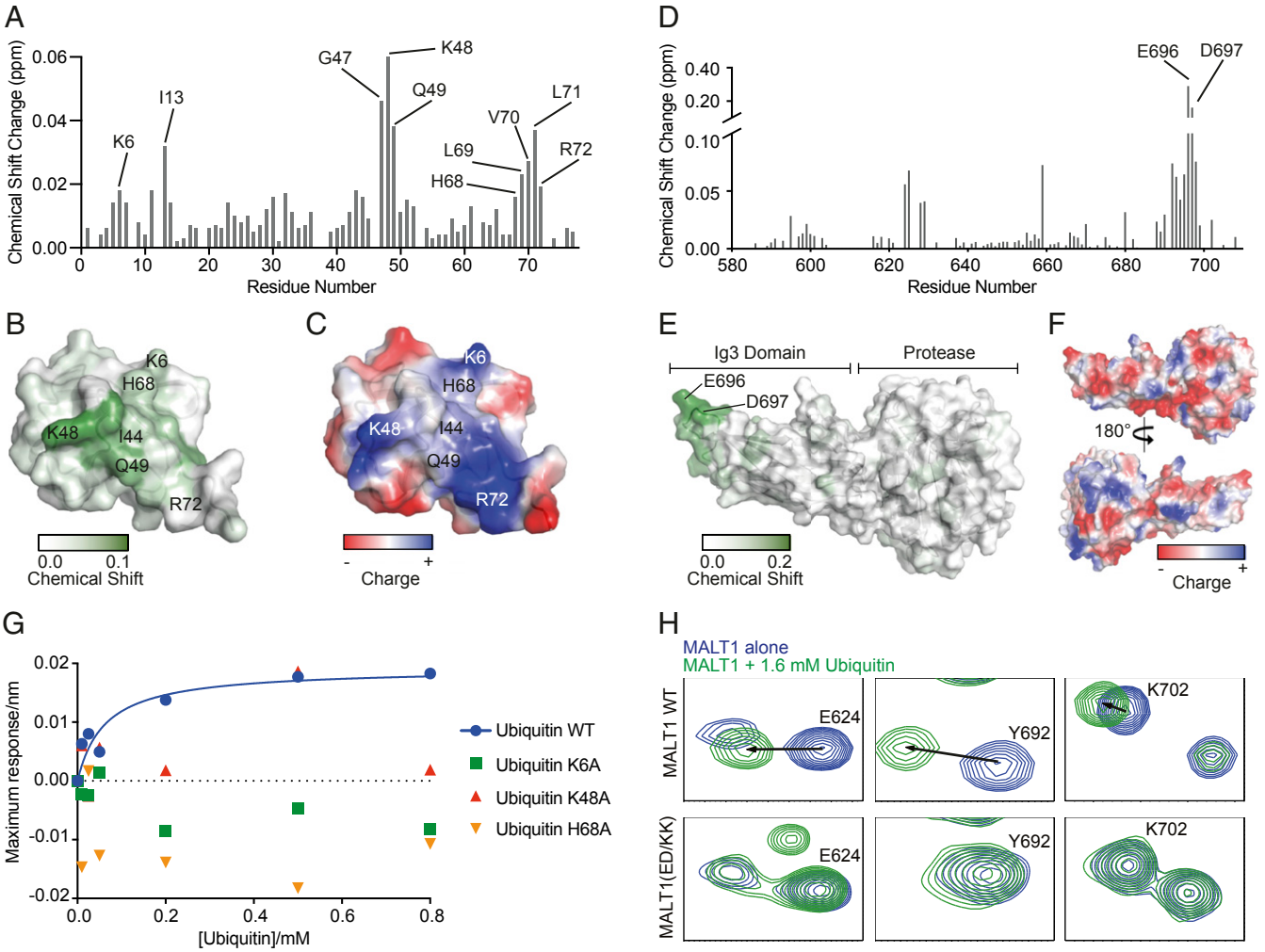

Fig. 1. Monomeric ubiquitin binds to the Ig3 domain of MALT1. (*A*) Backbone amide minimal shifts seen for ^{15}N-labeled human ubiquitin (residues 1–76) upon mixing with an over fivefold molar excess of purified MALT1 (residues 339–719). (*B*) Mapping of the minimal shift backbone amide NMR data onto a surface representation of ubiquitin with significantly perturbed residues (shift >0.01 ppm) colored with a gradient from white to green. Residues for which no minimal shift data were obtained are also shown in white. (*C*) An electrostatic surface representation of ubiquitin shown in the same orientation as *B* with areas of significant positive charge indicated in blue, and areas with negative charge indicated in red. Images in *B* and *C* were prepared using PyMOL. (*D* and *E*) As in *A* and *B*, showing backbone amide shifts seen for ^{15}N-labeled human MALT1 (residues 339–719) upon addition of an over 10-fold molar excess of human ubiquitin (residues 1–76). Data in *D* are only shown for amino acids constituting the Ig3 domain (580–709) as no significant changes were seen for backbone amide signals from residues in the MALT1 protease domain. (*F*) Surface charge representation of the MALT1 Ig3 and protease domains (positive charges are indicated in blue, and negative charges are indicated in red), highlighting the negatively charged surface around the region affected by ubiquitin binding. (*G*) MALT1 (residues 339–719) maximum binding response as a function of increasing concentrations of ubiquitin (residues 1–76) WT (blue filled circles), K6A (green filled squares), K48A (red filled upward triangles), and H68A (orange filled downward triangles). MALT1 WT binds to ubiquitin WT according to a one-site saturation-binding model with a dissociation constant (K_D) of ∼62.0 μM. No binding is detected between MALT1 WT and ubiquitin variants K6A, K48A, and H68A. (*H*) Highlighted backbone amide peaks from the ^{15}N-^{1}H TROSY spectra for E624, Y692, and K702, which show substantial shifts in MALT1 WT but not in MALT1(ED/KK) upon addition of ubiquitin.

binding of ubiquitin to the MALT1 Ig3 domain and gain insight into the underlying binding affinity, we used the Octet system (FortéBio) which measures interactions between purified proteins based on changes in light reflection from a protein-coated biosensor tip exposed to a protein-binding partner in solution. Under these conditions, ubiquitin bound to the MALT1 construct comprising the protease and Ig3 domains (residues 339–719), although with low affinity (~ 62 μM). Binding was lost upon mutation of residues within the positively charged surface patch of ubiquitin (K6A, K48A, or H68A) (Fig. 1*G*). Vice versa, wild-type (WT) ubiquitin was no longer able to induce changes in the $^{15}N/^{1}H$ TROSY spectrum of MALT1 when the negatively charged Ig3 residues E696 and D697 were mutated into lysine (MALT1(ED/KK)). Indeed, we observed a loss of ubiquitin-induced shifts in the backbone amide signals of several surrounding Ig3 residues, including E624, Y692, and K702 (Fig. 1*H* and *SI Appendix*, Fig. S1*C*). Collectively, these findings suggest that the surface residues E696 and D697 within the ubiquitin-interacting surface patch of the Ig3 domain physically interact with the positively charged surface area surrounding isoleucine 44 (I44) in ubiquitin.

The Ig3-Ubiquitin Interaction Is Required for Monoubiquitination-Dependent MALT1 Activation. We then mutated several of the Ig3 MALT1 residues identified by 2D-NMR to be involved in ubiquitin binding into alanine and assessed the effect of these point mutations on the catalytic activity of MALT1. For this, we used a previously described cellular MALT1 activity assay in which MALT1 is activated by coexpression of an oncogenic, constitutively active mutant of CARMA1, G116S (16), and protease activity is assessed using a previously described fluorescence resonance energy transfer (FRET)-based reporter assay (15). This assay is based on the MALT1-dependent cleavage of an eYFP-linker-eCFP construct containing the linker sequence LVSR, which is derived from the MALT1 substrate RelB (17). Cleavage of the linker causes a loss of FRET and gain in CFP fluorescence that can be quantified by flow cytometry (15). Using this assay, we found that mutation of I625 into alanine (I625A) led to an almost complete loss of activity (*SI Appendix*, Fig. S2*A*) that was comparable to the defect of a previously described monoubiquitination-deficient mutant K644R (15). However, when comparable plasmid concentrations were used for transfection, the I625A expression construct consistently showed reduced expression and solubility. The position of I625, which points toward the inside of the Ig3 domain, suggests that its mutation may lead to misfolding of the domain as the aliphatic side chain sits within a hydrophobic pocket formed by residues V598, Y692, P622, and Y690; we, therefore, excluded it from further analysis. Individual mutation of D595, E624, T698, and K702 into alanine did not reduce MALT1 activity, but mutation of Y692 or of both E696 and D697 into alanine (ED/AA) led to a partial or strong reduction, respectively, of MALT1 activity (Fig. 2*A* and *SI Appendix*, Fig. S2*A*). This reduction of activity was even more pronounced when the two negatively charged surface residues were mutated into lysine (ED/KK) (Fig. 2*A*).

Next, we assessed the functional consequences of the above-described perturbations of the ubiquitin-MALT1 interaction on the protease function of MALT1 in living cells. We first monitored the capacity of the ED/AA and ED/KK mutants to cleave RelB and CYLD, two known MALT1 substrates with inhibitory roles in the NF-κB and AP-1 transcriptional pathways, respectively (17, 18). Cleavage of RelB and CYLD was easily induced upon their coexpression with oncogenic CARMA1 and WT MALT1 in 293T cells (Fig. 2*B* and *SI Appendix*, Fig. S2*B*). The cleavage of these substrates was entirely or strongly impaired when using catalytically inactive (C464A) or monoubiquitination-deficient (K644R) MALT1 mutants, respectively (Fig. 2*B* and *SI Appendix*, Fig. S2*B*). Mutation of the E696/D697 residues into AA or KK led to a partial or strong reduction of substrate cleavage, respectively (Fig. 2*B* and *SI Appendix*, Fig. S2*B*).

To gain insight into the reasons underlying the reduced catalytic activity of the ED/KK mutant of MALT1, we next assessed its status of monoubiquitination, which we had previously identified as an important hallmark of MALT1 activation. In 293T cells, MALT1 monoubiquitination can be induced by coexpression of MALT1 with its binding partner BCL10 (15). In this system, the ubiquitin-binding-deficient ED/KK mutant showed a dramatically decreased capacity to become monoubiquitinated (Fig. 2*C*). To test whether mutation of the ED motif affected MALT1 monoubiquitination in T cells, we stably expressed various MALT1 constructs in a MALT1-deficient Jurkat T cell line. In these cells, MALT1 becomes monoubiquitinated on K644 as a consequence of cellular stimulation with phorbol myristate acetate (PMA) and the calcium ionophore ionomycin (mimicking strong T cell activation) (15). In stimulated cells, monoubiquitination was, indeed, detectable for WT and catalytically inactive (C464A) MALT1 but absent for the monoubiquitination-deficient K644R mutant as reported (15) (Fig. 2*D*). The ubiquitin-binding deficient ED/AA and ED/KK mutants showed impaired monoubiquitination (Fig. 2*D*). This suggests that ubiquitin binding by the Ig3 domain is required for MALT1 monoubiquitination, possibly in a manner that is similar to what has been shown for other ubiquitin-binding proteins (19, 20). Thus, via the ubiquitin-binding Ig3 domain, MALT1 may promote its own monoubiquitination by recruiting a ubiquitin-charged E2 or E3 enzyme that remains to be identified.

The Ig3-Ubiquitin Interaction Is Required for MALT1-Dependent T Cell Activation. To explore the biological consequences of perturbing the Ig3-ubiquitin interactions, we analyzed the effect of corresponding MALT1 mutants on T cell activation. For this purpose, we first silenced endogenous expression of MALT1 by CRISPR-mediated gene targeting in Jurkat T cells and then reconstituted the cells with various MALT1 mutants (Fig. 2*E* and *SI Appendix*, Fig. S2*C*). We then assessed diverse readouts of MALT1-dependent T cell activation upon stimulation of the Jurkat T cells with PMA and ionomycin. To assess MALT1 protease activity, we monitored the stimulation-induced cleavage of the MALT1 substrates CYLD and Roquin-1. As expected, we saw a complete or strong reduction of substrate cleavage for the cells reconstituted with the catalytically inactive (C464A) or monoubiquitination-deficient (K644R) mutants. The E696 and D697 mutants, ED/AA and ED/KK, showed a partial reduction of substrate cleavage (Fig. 2*E*). Stimulation-induced phosphorylation of the NF-κB inhibitor IκBα and activation of the c-Jun N-terminal kinase (JNK) pathway, which can be assessed by monitoring JNK phosphorylation, depends only on the scaffold function of MALT1 (3, 4, 6, 17, 21). Neither phosphorylation of IκBα nor activation of JNK was affected by ED/AA or ED/KK mutation (Fig. 2 *D* and *E*). This indicates that the identified ubiquitin-binding domain of MALT1 is necessary for its protease function but not for its scaffold function. The scaffold function of MALT1 requires its interaction with the ubiquitin ligase TRAF6, which mediates the recruitment and activation of the IκB kinase (IKK) complex to promote the phosphorylation and subsequent degradation of the NF-κB inhibitor IκBα (22–24). Consistent with an unaltered capacity to support IκBα and JNK phosphorylation, the MALT1 mutants ED/AA, ED/KK, and the ubiquitination-deficient MALT1 mutant K644R were still able to interact with TRAF6 upon coexpression in 293T cells (*SI Appendix*, Fig. S2*D*), in contrast to a MALT1 construct (E3A) mutated in three previously reported TRAF6-binding sites (22, 23). Thus, disrupting the region mediating the ubiquitin-MALT1 interaction impaired MALT1-dependent substrate cleavage in vivo but did not affect the scaffold function of MALT1.

Finally, we monitored the effect of MALT1 ED/AA and ED/KK mutants on the stimulation-induced transcription and

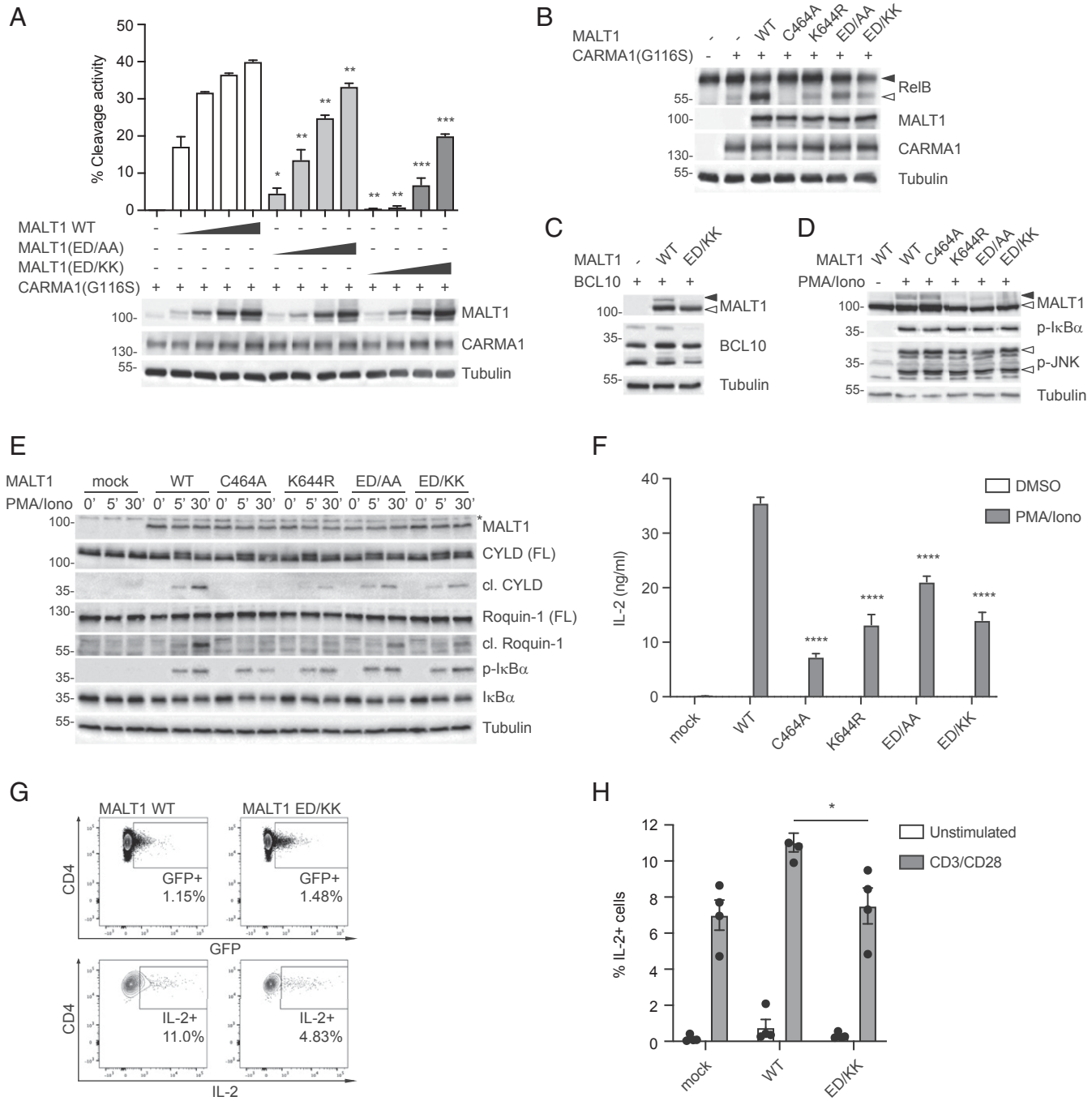

Fig. 2. The Ig3-ubiquitin interaction is required for monoubiquitination-dependent MALT1 activation and T cell function. (*A* and *B*) Assessment of MALT1-dependent FRET reporter cleavage (*A*) or RelB cleavage (*B*) in 293T cells. The reporter or RelB were coexpressed with oncogenic CARMA1(G116S) and WT MALT1 or the indicated MALT1 mutants of E696 and D697 (ED/AA or ED/KK). FRET reporter cleavage was assessed by flow cytometry (*A*) and protein expression, and RelB cleavage was assessed by Western blot as indicated (*A* and *B*). Positions of uncleaved (black arrowhead) and cleaved (open arrowhead) RelB are indicated. (*C*) HEK 293T cells were transfected with the indicated expression constructs for MALT1 and BCL10 and analyzed for MALT1 monoubiquitination by Western blot as indicated. Positions of monoubiquitinated MALT1 (black arrowhead) and unmodified MALT1 (open arrowhead) are indicated. Multiple bands in the BCL10 blot correspond to previously described phosphorylation isoforms (39). (*D*) MALT1-deficient Jurkat T cells were reconstituted with the indicated MALT1 constructs and incubated for 1 h with the MALT1 active site inhibitor z-LVSR-fmk before stimulation with PMA and ionomycin for 1 h. MALT1 monoubiquitination, phosphorylation of IκBα, and phosphorylation of JNK were analyzed by Western blot. (*E*) MALT1-deficient Jurkat T cells reconstituted with the indicated empty vector (mock) or MALT1 constructs were stimulated with PMA and ionomycin for 0, 5, or 30 min. Substrate cleavage (CYLD and Roquin-1) and phosphorylation of IκBα were analyzed by Western blot. Tubulin was used as a loading control, and positions of molecular weight markers (in kDa) are indicated (*A*–*E*). (*F*) IL-2 secretion of MALT1-deficient Jurkat T cells reconstituted with the indicated MALT1 constructs, stimulated for 16 h with PMA and ionomycin or solvent alone. (*G* and *H*) Analysis of intracellular IL-2 in isolated primary $CD4^+$ T cells from four healthy donors, lentivirally transduced with mock, MALT1 WT, or MALT1(ED/KK) constructs and stimulated with anti-CD3, anti-CD28, and a cross-linking antibody in the presence of brefeldin A. The percentage of $IL\text{-}2^+$ cells among infected GFP^+ cells was determined by flow cytometry. (*G*) Gating strategy for one donor for MALT1 WT and MALT1(ED/KK) transduced cells. (*H*) Combined analysis of four donors. Bars represent means ± SD (*A* and *F*) or means ± SEM (*H*); $*P < 0.05$, $**P < 0.01$, $***P < 0.001$, and $****P < 0.0001$. Data are representative of three (*A*–*D*), two (*E*), and four (*F* and *H*) experiments.

secretion of the cytokine IL-2, a major NF-κB target, in Jurkat T cells and primary human T cells. Similar to the catalytically inactive form of MALT1 (C464A), the monoubiquitination-deficient (K644R) or ubiquitin-binding-deficient (ED/KK) MALT1 mutants showed a strong impairment of their capacity to support the transcription and secretion of IL-2 in Jurkat T cells, an effect that was less pronounced for the ED/AA mutant (Fig. 2*F* and *SI Appendix*, Fig. S2*E*). The residual transcription and secretion of IL-2 observed with the catalytically inactive mutants in these assays are due to their remaining scaffold functions (15, 25). Finally, we transduced purified primary human CD4 T cells with lentiviral expression vectors for MALT1 and GFP and assessed the capacity of the transduced GFP-positive T cells to produce IL-2 by flow cytometry. In transduced T cells from four independent healthy donors, we observed that the ED/KK mutant was significantly impaired in its capacity to support stimulation-induced IL-2 production compared to WT MALT1 (Fig. 2 *G* and *H*). Thus, the intact ubiquitin-interaction surface of the Ig3 domain is required for optimal MALT1-dependent T cell activation.

The Ubiquitin-Binding Deficient Ig3 Mutants Can Still Be Activated by Functional Ubiquitin. So far, our data suggested that the Ig3 domain binds ubiquitin for the purpose of its conjugation to MALT1, but it remained unclear whether the ubiquitin-binding site in the Ig3 domain was also required to mediate the activating effect of MALT1 monoubiquitination. We have previously shown that MALT1 can be artificially activated by the generation of a MALT1-ubiquitin (MALT1-Ub) fusion protein that mimics monoubiquitination by covalent attachment of ubiquitin to the MALT1 C terminus and that this fusion overcomes the catalytic defect of the ubiquitination-deficient K644R mutant (15). Therefore, we next assessed whether introduction of the ubiquitin-binding-deficient Ig3 mutations would affect the activity of the MALT1(K644R)-Ub constructs. Indeed, neither the ED/AA nor the ED/KK mutations affected the activity of the MALT1(K644R)-Ub, suggesting that monoubiquitin, once covalently attached to MALT1, promotes MALT1 activation in a manner that is independent of the ubiquitin-binding site in the Ig3 domain (Fig. 3*A*). Next, we assessed the capacity of ubiquitin to induce MALT1 activation in a different in vitro setting in which MALT1 activity is monitored by the fluorogenic cleavage of the optimal tetrapeptide substrate LVSR-amc (25, 26). We observed that purified recombinant ubiquitin can activate purified recombinant MALT1 (aa 199–824) in a dose-dependent manner (*SI Appendix*, Fig. S3*A*) and that this required the presence of the hydrophobic ubiquitin surface residue I44 (*SI Appendix*, Fig. S3*B*) (27).

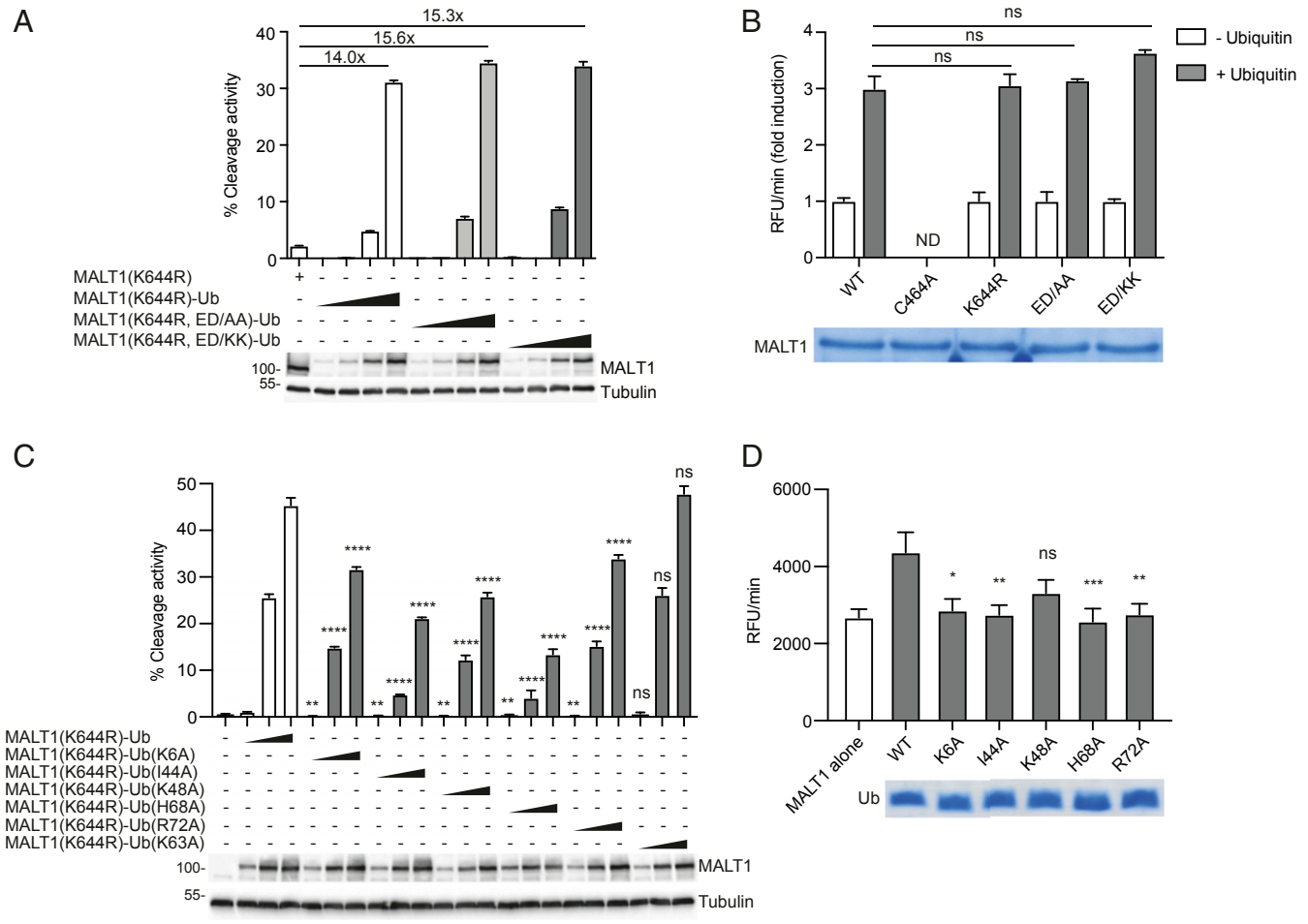

Fig. 3. The ubiquitin-binding deficient Ig3 mutants can still be activated by functional ubiquitin. (*A* and *C*) Flow cytometric assessment of MALT1-dependent FRET reporter cleavage in 293T cells. The reporter was coexpressed with the indicated MALT1-ubiquitin fusion constructs. Protein expression was controlled by Western blotting as indicated. Positions of molecular weight markers (in kDa) are indicated. (*B* and *D*) In vitro cleavage activity of indicated recombinant purified MALT1 constructs (residues 199–824, 0.6 μM) in the absence or presence of recombinant purified ubiquitin constructs (0.1 mM). Protein amount was controlled by Coomassie-blue staining as indicated. Data are representative of two experiments (*A*–*D*). Bars represent means ± SD; ns, nonsignificant, $*P < 0.05$, $**P < 0.01$, $***P < 0.001$, and $****P < 0.0001$.

Importantly, in this system, ubiquitin cannot be covalently linked to K644 of MALT1, so to reach detectable MALT1 cleavage activity, high concentrations of free monoubiquitin have to be added. To test whether ubiquitin could still activate the ubiquitin-binding-deficient MALT1 Ig3 mutants, we generated these in recombinant purified form and tested their activity in the absence and presence of recombinant monoubiquitin. Under these conditions, and similar to our previous observations in the in vivo system, we found that addition of free ubiquitin was still able to activate both the ubiquitin conjugation- and the ubiquitin-binding-deficient MALT1 mutants (Fig. 3*B*). Thus, binding of the Ig3 domain to ubiquitin serves to promote monoubiquitination, but upon its covalent attachment in vivo (Fig. 3*A*) or addition in excess in vitro (Fig. 3*B* and *SI Appendix*, Fig. S3*A*), ubiquitin promotes MALT1 activation by additional means.

We next assessed whether mutations of four positively charged ubiquitin residues, K6, K48, H68, and R72, which are located close to I44, affected the capacity of ubiquitin to activate MALT1 upon their fusion to the C terminus of MALT1. At comparable levels of expression, we observed that mutation of I44, but also of the positively charged surface residues K6, K48, H68, and R72, reduced the capacity of the C-terminally fused ubiquitin to promote MALT1-dependent FRET reporter cleavage in 293T cells (Fig. 3*C*). In contrast, mutation of K63 to alanine, which is not located on the positively charged surface surrounding I44, had no effect on the cleavage activity of the MALT1-Ub fusion protein (Fig. 3*C*). Next, we monitored the capacity of recombinant purified ubiquitin constructs with these mutations to activate recombinant purified MALT1 in vitro. This revealed that mutation of I44 or of the four surrounding positively charged residues, K6, K48, H68, and R72 also impaired the capacity of free ubiquitin to activate MALT1 (Fig. 3*D*). Together with the results obtained in Fig. 1, these findings suggest that the positively charged ubiquitin surface surrounding I44, incorporating residues K6, K48, H68, and R72, is important for both its recruitment by the Ig3 domain and subsequent conjugation to K644 and for the subsequent monoubiquitin-dependent activation of MALT1.

Mutation of Y657 Induces Coordinated Conformational Changes in the Loop Connecting K644 to Y657 and the Active Site. The comparison of MALT1 crystal structures in the absence (PDB: 3V55) and presence (PDB: 3UO8) of a peptide inhibitor and substrate analog z-VRPR-fmk suggests that substrate binding induces a rotational movement of the protease domain with respect to the Ig3 domain (13). In the peptide-bound conformation, Y657 on the Ig3 domain forms a hydrogen bond with E368 and hydrophobic interactions with Y367 and L506, located on the surface of the protease domain (14) (Fig. 4*A*). Whether these interactions are relevant to the activation of MALT1 by monoubiquitination remains unknown. In our hands, addition of free ubiquitin did not show noticeable effects on backbone amide signals in this region (Fig. 1*D* and *SI Appendix*, Fig. S1*B*). However, the NMR approach relied on the use of monomeric MALT1 and free (not K644-attached) ubiquitin. Since the active form of MALT1 has been proposed to be a dimer (13, 14, 28), our approach is likely to miss additional conformational changes that could be induced by interactions of ubiquitin with MALT1 dimers as well as pulling or pushing forces that might be exerted by ubiquitin on the Ig3 domain as a result of its covalent attachment to K644. We reasoned that the latter may structurally alter the loop extending from K644 to Y657 and thereby potentially affect the previously reported hydrophobic interactions between residues Y657 on the Ig3 domain and L506 and Y367 in the protease domain, which are dramatically altered upon binding of the substrate analog z-VRPR-fmk (14) (Fig. 4*A*).

To test the proposed model, we next assessed the activity and structure of a Y657A MALT1 mutant in vitro. In the absence of ubiquitin, the Y657A mutant was hyperactive compared to WT MALT1. Addition of ubiquitin led to a significant increase in the activity of WT MALT1 but had no significant impact on the activity of the hyperactive Y657A mutant (Fig. 4*B*). Thus, a mutational disruption of the Ig3-protease interaction rendered this mutant independent of ubiquitin-mediated activation. Consistent with this idea, the MALT1 Y657A mutant also no longer depended on ubiquitination-dependent activation through oncogenic CARMA1 in vivo (Fig. 4*C* and *SI Appendix*, Fig. S4*A*). To further probe the conformational effect of the Y657A mutation on MALT1 and to potentially understand how attachment of ubiquitin at K644 might be coupled to conformational changes at the Ig3-protease interface leading to the activation of the protease, a $^{15}N/^{1}H$ TROSY spectrum of uniformly labeled MALT1 Y657A (339–719) was collected and compared with the spectrum of the WT form of MALT1 (*SI Appendix*, Fig. S4 *B* and *C*). It should be noted that, due to the overlapped nature of peaks within the $^{15}N/^{1}H$ TROSY spectrum of MALT1, which contains backbone amide signals from over 365 residues, the minimal shift analysis presented here is a conservative method for determining residues that have undergone significant chemical shift perturbations due to the Y657A substitution, so some of the affected residues may not be identified. Comparing the $^{15}N/^{1}H$ TROSY spectra of WT MALT1 with MALT1 Y657A revealed that this single point mutation led to a significant number of chemical shift perturbations within both the Ig3 and the protease domains (Fig. 4 *D* and *E* and *SI Appendix*, Fig. S4 *C* and *D*), which extended beyond the region immediately surrounding the mutated residue. In particular, several of the residues in the loop region linking Y657 to K644 had chemical shift perturbations greater than 0.05 ppm (Fig. 4*E*), including D645, N647, K648, T650, E652, T654, and S656, suggesting the possibility of signal transfer between K644 and Y657 upon ubiquitin attachment. A number of residues within the protease domain also experienced very significant chemical shift perturbations (Fig. 4 *D* and *E* and *SI Appendix*, Fig. S4*D*), including L363, V364, Y367, and E368, located in the α1-helix of the protease domain directly adjacent to Y657A. More interestingly, some of the residues that line the substrate binding groove within the protease domain were also affected, including A413, H415, C464, and E497 (Fig. 4*D* and *SI Appendix*, Fig. S4*D*). These findings suggest that the Y657A mutation impacts on the conformation of residues surrounding the active site. Thus, ubiquitin conjugation to K644 likely drives a conformational change in the loop containing Y657, which leads to protease activation by changing the conformation and/or mobility of residues surrounding the hydrophobic Ig3-protease interface and active site region. The dramatic hyperactivation of the protease produced by the Y657A mutation and its uncoupling of activation from ubiquitin modification of K644 clearly highlights Y657 as a key mediator of signaling between the Ig3 and the protease domains of MALT1 through a series of concerted conformational changes.

Mutants That Disturb the Ig3-Protease Interaction Activate MALT1 and Overcome Defects in Ubiquitin-Dependent MALT1 Activation. To probe the idea that mutational disruption of the hydrophobic Ig3-protease interaction surface was a key determinant in MALT1 activation, we mutated several additional amino acids involved in these interactions, namely, L506, N508, and Y367 (13, 14). Mutation of these residues into alanine showed a dramatic activation of MALT1 in the absence of ubiquitination-promoting expression of oncogenic CARMA1 (Fig. 4*F*). For L506, the hyperactivation was even more dramatic when L506 was mutated into glycine (L506G) or lysine (L506K). Almost no activating effect was observed upon mutation of Y657 into phenylalanine (Y657F), which should maintain the possibility of hydrophobic interactions (Fig. 4*F*) but destroys the possibility of a hydrogen bond between Y657 and E368, suggested by the MALT1 crystal structure (14). Thus, disruption of a group of hydrophobic Ig3-protease interactions led to constitutive activation of MALT1. The activity of WT MALT1 and the Y657F mutant could be

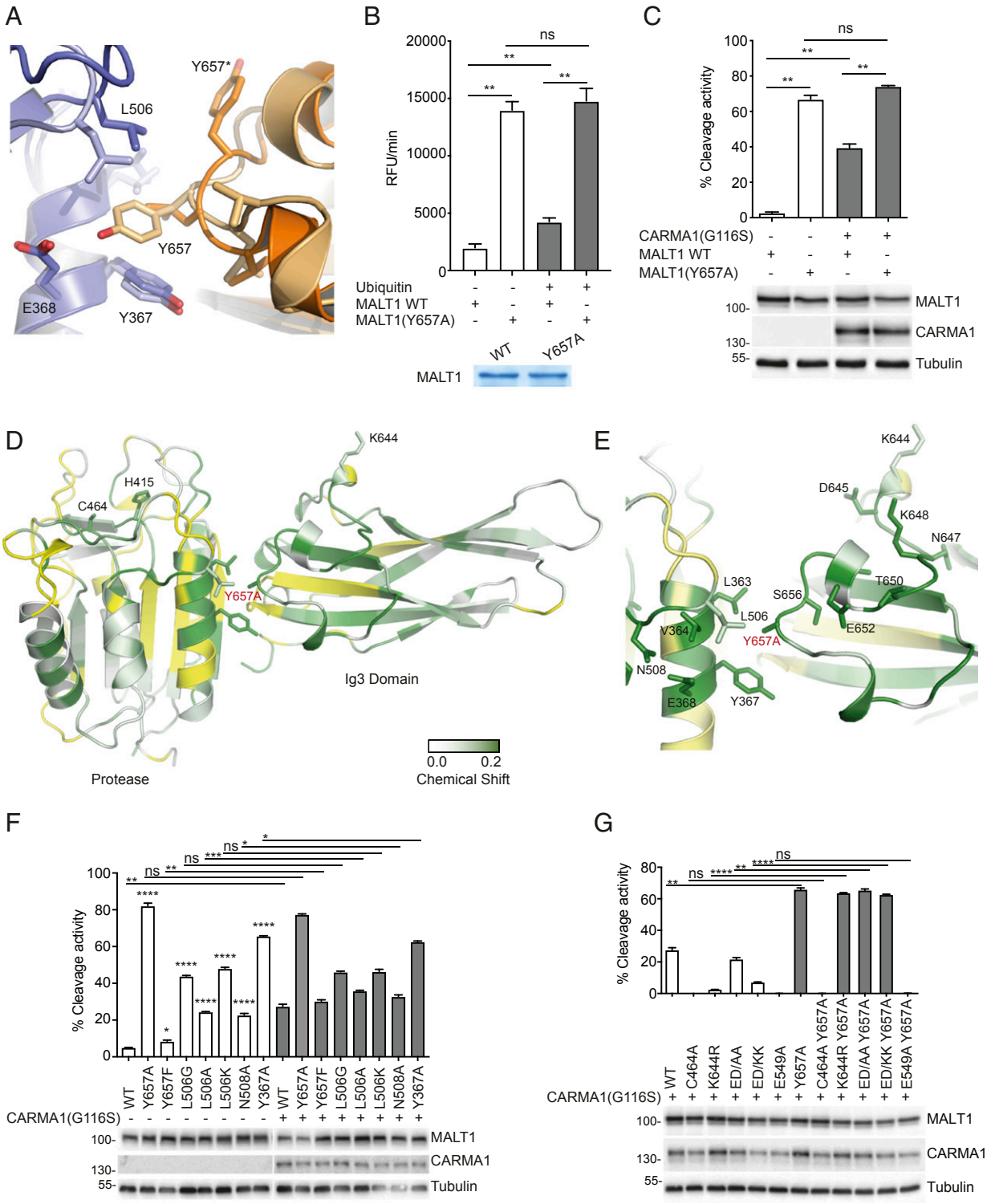

Fig. 4. Mutation of Y657 induces coordinated conformational changes in the loop connecting K644 to Y657 and the active site. (*A*) Overlay of the MALT1 Ig3-protease interface from reported crystal structures, which shows a major conformational switch of Y657 in the presence (light orange/light blue [PDB: 3UO8]) and the absence (dark orange/dark blue [PDB: 3V55]) of the active site peptide inhibitor z-VRPR-fmk. Blue and orange colors represent the protease and Ig3 domains, respectively. (*B*) In vitro cleavage assay comparing the capacity of ubiquitin (0.1 mM) to activate WT MALT1 or a MALT1 Y657A mutant (residues 199–824, 0.6 μM). Protein amount was controlled by Coomassie-blue staining as indicated. (*C*) Flow cytometric assessment of MALT1-dependent FRET reporter cleavage in 293T cells. The reporter was coexpressed with the indicated MALT1 constructs together with oncogenic CARMA1(G116S). Protein expression was controlled by Western blotting as indicated, and positions of molecular weight markers (in kDa) are indicated (*C*). (*D* and *E*) Backbone amide chemical shift changes induced by the Y657A mutation in MALT1 and mapped onto the reported structure of the Ig3-protease domains. Residues with significantly perturbed NMR signals (shift > 0.01 ppm) are colored with a gradient from white to green. Residues for which no minimal shift data were obtained are shown in yellow. Figure prepared using PyMOL. Residues with clearly shifted signals located at the Ig3-protease interface are highlighted (*E*). (*F* and *G*) Cleavage activity of the indicated MALT1 constructs was assessed as in *C*. Data are representative of two (*C*, *F*, and *G*) or three (*B*) experiments. Bars represent means ± SD; ns, nonsignificant, $*P < 0.05$, $**P < 0.01$, $***P < 0.001$, and $****P < 0.0001$.

further boosted by ubiquitination-promoting coexpression of oncogenic CARMA1. In contrast, oncogenic CARMA1 had no or little effect on the activity of the hyperactive L506A, L506G, L506K, N508A, and Y367A mutants, suggesting that their activity was no longer dependent on ubiquitination (Fig. 4*F*). Importantly, the Y657A mutation was also able to fully rescue the catalytic defect of the ubiquitination-deficient K644R mutant but not of the catalytically inactive C464A mutant (Fig. 4*G* and *SI Appendix*, Fig. S5). Similarly, introduction of the Y657A mutation into the functionally impaired ED/AA or ED/KK mutants fully restored their catalytic activity (Fig. 4*G*). Of note, the Y657A mutant was unable to restore the activity of a previously described dimerization-deficient MALT1 mutant in which E549 in the protease–protease interface has been mutated into alanine (E549A) (28) (Fig. 4*G*). Collectively, these findings suggest that ubiquitin attachment to K644 promotes a perturbation of the Ig3-protease interface, which is communicated to the active site through subtle conformational changes to promote MALT1 activation.

Discussion

Here, we identify the Ig3 domain of MALT1 as a novel ubiquitin-binding motif that is essential for MALT1 activation through an allosteric mechanism. Our data support a model in which the Ig3 domain recruits ubiquitin to promote MALT1 monoubiquitination, which, in turn, leads to disruption of the hydrophobic Ig3-protease interface and induces conformational changes in the protease domain that increase MALT1 activity (Fig. 5). Using a combination of heteronuclear NMR studies, mutational, and biochemical approaches, we show that ubiquitin binds the Ig3 domain via a negatively charged surface patch including E696 and D697 that is located on the side opposing the Ig3-protease domain interaction surface. We also provide relevant insight into how ubiquitin promotes MALT1 activation. MALT1-binding induced shifts in ubiquitin backbone amide signals for a total of 13 amino acids forming a continuous positively charged patch on the surface of ubiquitin. These residues are likely to be important for ubiquitin recruitment by the Ig3 domain, but also for the capacity of ubiquitin to activate MALT1 upon its covalent conjugation to MALT1. In support of this, we found that mutation of several of the positively charged ubiquitin residues important for MALT1 binding were impaired in their capacity to promote MALT1 activation in vitro or in the context of a MALT1-Ub fusion protein. Thus, the same positively charged ubiquitin surface surrounding I44 is likely to be required for both Ig3-dependent ubiquitin binding/conjugation and for the subsequent MALT1 activation by K644-conjugated ubiquitin, which likely depends on an interaction of ubiquitin with a MALT1 surface that was not accessible in the in vitro NMR system used here. Indeed, for the 2D-NMR analysis, recombinant MALT1 needs to be monomeric in solution, and, under these conditions, free ubiquitin did not show noticeable effects on backbone amide signals in the protease domain or the protease-Ig3 interface. However, under the conditions of the assay used for monitoring its activity and in vivo, MALT1 is most likely active as a dimer or oligomer and/or adapts a different conformation. We, therefore, suspect that MALT1 contains a second cryptic ubiquitin-binding site that may be exposed only upon a specific conformational change or dimerization of MALT1. Consistent with the latter idea, we found that a Y657A mutation, which overcomes the need for monoubiquitination-dependent activation, was unable to activate a dimerization-deficient MALT1 mutant (E549A). Future studies will be targeted at elucidating how K644-conjugated ubiquitin activates dimeric MALT1.

We reasoned that, independent of the exact MALT1-binding site of K644-conjugated ubiquitin, such a binding could exert a mechanical force on K644 that might structurally order the loop extending from K644 to Y657. This could, in turn, disrupt the previously reported hydrophobic interaction between L506 and Y657 (14) and thereby affect the position of the A491–A507 loop

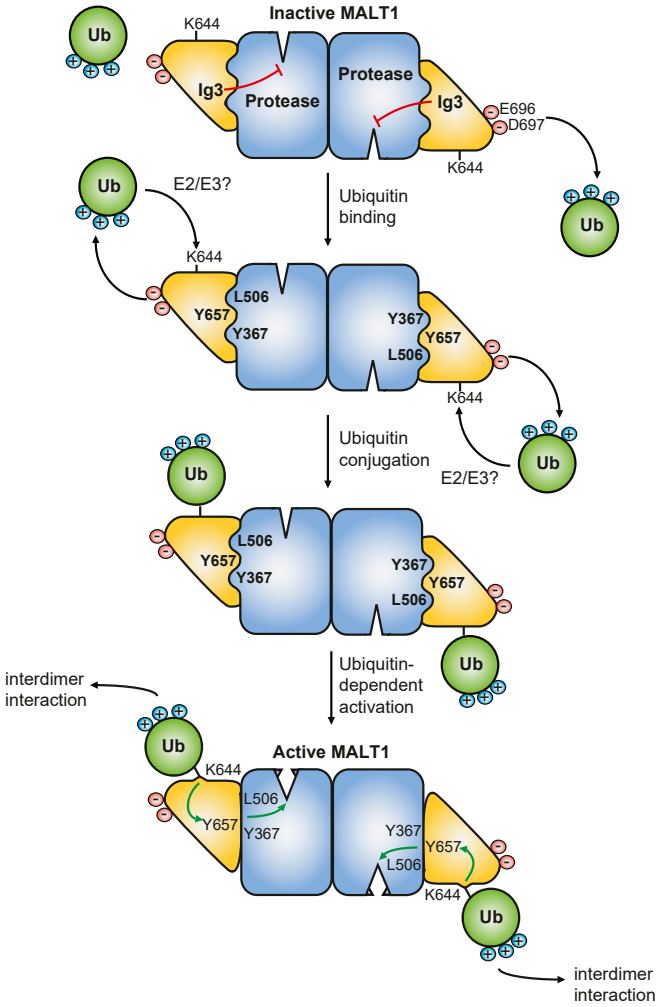

Fig. 5. Hypothetical model for allosteric MALT1 activation. In the inactive form, the Ig3 domain interacts with the protease domain via a hydrophobic interaction comprising Y657 on the surface of the Ig3 domain and L506 and Y367 on the surface of the protease domain. The negatively charged residues E696 and D697 of the Ig3 domain are necessary for the recruitment and conjugation of ubiquitin to K644 of the Ig3 domain via unknown E2/E3 enzymes. Upon conjugation to K644, ubiquitin likely interacts with an additional unknown ubiquitin-binding site of an adjacent MALT1 dimer. This induces a conformational change in the Ig3 domain that perturbs the hydrophobic Ig3-protease interaction thereby allowing the adoption of a catalytically active conformation.

within the protease domain. In support of this hypothesis, mutation of tyrosine 657 into alanine (Y657A) led to the creation of a hyperactive MALT1 mutant, which no longer depended on ubiquitination and the Ig3-ubiquitin interaction for its activation. Moreover, our 2D-NMR analysis revealed that the Y657A mutation, indeed, caused major chemical shift perturbations, both in the loop extending from Y657 to K644 and in the protease domain, including the active site residues H415 and C464. This supports the idea that the ubiquitin-conjugation site K644 and the Y657-surrounding Ig3-protease interaction sites communicate. Based on these findings, we propose that the interaction of K644-conjugated ubiquitin with an unknown ubiquitin-binding site on an adjacent MALT1 dimer activates the protease domain of the monoubiquitinated subunit by inducing a Y657-dependent change in the interaction of the Ig3 and protease domains, which lock MALT1 in its active conformation (Fig. 5).

Several studies have reported the development of MALT1 inhibitors with efficacy as immunomodulating or anticancer drugs in

mouse models of autoimmunity and lymphomas (29–31). Inhibition of MALT1 function preferentially in Treg cells, on the other hand, may reprogram these cells to become proinflammatory effectors (32–34) that sensitize tumors to the PD-1 blockade in mouse tumor models (32). Whether these approaches work similarly in humans and in mice remains unknown and requires further investigation. MALT1 inhibitors are either irreversible inhibitors that target the active site (30, 35, 36) or compounds that bind to an allosteric site located near W580 between the Ig3 and the protease domains and thereby prevent the conformational change required to form the active conformation (29, 37, 38). Our findings suggest that it should be possible to induce MALT1 activity in a reversible manner using drugs that interfere with the Ig3-protease interaction in the hydrophobic region surrounding Y657. Such drugs could be desirable to treat certain forms of severe immunodeficiencies or to strengthen antitumor immune responses, for example, by pretreatment of chimeric antigen receptor-T cells or other immune cells to be used for adoptive cancer immunotherapies.

Materials and Methods

Antibodies and Plasmids. Details about antibodies and plasmids are provided in the *SI Appendix*.

Transfection and Transduction of Cells. Transient transfection of HEK293T cells and lentiviral transduction of Jurkat T cells have been previously described (25). To silence MALT1 expression, cells were stably transduced with a MALT1-specific single guide RNA (sgRNA) (5′-GCTGTTGGGGGACCCGCTAC-3′) or control sgRNA (5′-CTTCGAAATGTCCGTTCGGT-3′) and selected using puromycin. Cells were subsequently transduced to constitutively express GFP together with WT or mutant MALT1 constructs that were rendered CRISPR/Cas9 resistant by a silent point mutation. Transduced cells were sorted for live GFP+ cells using flow cytometry.

Cell Culture, Cell Stimulation, and IL-2 Luciferase Reporter Assays. HEK293T cells and Jurkat T cells were cultured in DMEM or in Roswell Park Memorial Institute (RPMI)-1640 medium supplemented with 10% fetal calf serum (FCS) (Biowest), respectively. Lentivirus-transduced Jurkat T cells were kept under puromycin selection (1 μg/mL; Alexis) for 14 d. For stimulation of T cells, a mixture of PMA (phorbol 12-myristate 13-acetate; 20 ng/mL; Alexis) and ionomycin (1 μM; Calbiochem) was used. In some experiments, cells were preincubated with z-LVSR-fmk (2 μM; Bachem) for 30–60 min before stimulation of Jurkat T cells or treated for 16 h after transfection of HEK293T cells. IL-2 luciferase reporter assay was performed as previously described (17, 25).

Lysis, Immunoprecipitation, and Immunoblot Analysis. Cells were lysed in lysis buffer containing 50 mM 4-(2-hydroxyethyl)-1-piperazineethanesulfonic acid (Hepes) pH 7.5, 150 mM NaCl, 1% Triton-X-100, protease inhibitors (Complete; Roche), and phosphatase inhibitors (NaF, $Na_4P_2O_7$, and Na_3VO_4). For optimal detection of MALT1 monoubiquitination, the lysis buffer was supplemented with *N*-Ethylmaleimide (10 mM). After preclearing the lysates with Sepharose beads for 20 min, StrepTactin Sepharose beads (IBA Lifesciences) were added, and samples were incubated for 1 h at 4 °C. The samples were then washed three times with lysis buffer. Samples were boiled in a reducing sodium dodecyl sulfate (SDS) sample buffer, separated by SDS/polyacrylamide gel electrophoresis, and analyzed by immunoblot as described (25).

CD4+ T Cell Isolation from Blood Samples and Intracellular IL-2 Staining. Blood samples from healthy, informed and consenting donors were obtained from the Interregional Blood Transfusion SRC Ltd. Peripheral blood mononuclear cells were isolated by density centrifugation with Lymphoprep. CD4+ T cells were obtained using CD4 MicroBeads from Miltenyi and cultivated in RPMI-1640 medium supplemented with 10% FCS (Biowest), 1% penicillin/streptomycin, and IL-2 (100 U/mL). One day before lentiviral transduction, cells were primed with anti-CD3, anti-CD28 (Biolegend), and a cross-linking antibody (Jackson Immunoresearch) (1 μg/mL of each). Lentiviral transduction was performed in the presence of 6 μg/mL polybrene and a centrifugation of the cell-virus mix for 90 min at 800 g at 32 °C. After 2.5 d, cells were washed three times with fresh medium and cultivated in the presence of IL-2 for 1 wk. Further on, cells were restimulated with anti-CD3, anti-CD28 (0.5 μg/mL of each), and a cross-linking antibody (1 μg/mL) for 6 h in the presence of brefeldin A (eBioscience). All cells were stained for CD4 using an APC anti-human CD4 (SK3) antibody from BioLegend. Dead cells were stained with eBioscience Fixable Viability Dye eFlour 506 (Invitrogen). After fixation in 4% paraformaldehyde and permeabilization in 0.1% Saponin, intracellular IL-2 was stained by PE-CF594 Mouse Anti-Human IL-2 (5344.111) from BD Biosciences. The percentage of IL-2-positive cells was determined using a LSRIIb flow cytometer from BD Biosciences.

Protein Purification and In Vitro Protease Activity Assay. Recombinant glutathione *S*-transferase proteins containing the MALT1 Ig2, protease, Ig3 domains, and the C-terminal extension (aa 199–824, 0.6 μM), or monomeric ubiquitin, were generated and purified as previously described (25). To measure protease activity in vitro in the presence of purified monomeric ubiquitin, samples containing purified MALT1 constructs were incubated in cleavage buffer (20 mM Hepes, 10 mM KCl, 1.5 mM $MgCl_2$, 1 mM ethylenediaminetetraacetic acid, 1 mM dithiothreitol, 0.01% Triton X-100, and 10% glycerol, pH 7.5) containing 200 μM of the fluorescent substrate Ac-LVSR-amc (Peptides International) for 4 h at 30 °C, and the protease activity of MALT1 was monitored using a microplate reader (Molecular Devices).

Minimal Shift Analysis Using NMR Spectroscopy. Recombinant MALT1 (residues 339–719), MALT1 E696K/D697K, MALT1 Y657A, and ubiquitin (residues 1–76) were expressed and purified as described in the *SI Appendix*. All NMR data were acquired on a Bruker Avance III 800 MHz spectrometer equipped with a 5 mm HCN cryoprobe. Experimental parameters and data acquisition times for each experiment are described in the *SI Appendix*. All NMR data were processed and analyzed using TopSpin and SPARKY (University of California, San Francisco) software.

Ubiquitin-MALT1-Binding Determination by Biolayer Interferometry. The dissociation constant (K_D) for MALT1 binding to ubiquitin was determined by biolayer interferometry on a two-channel Octet RED384 system (FortéBio). Protein samples were diluted in 1× HBS-EP+ buffer (GE Healthcare), and experiments were carried out at 25 °C and 1,000 rpm constant shaking. Ni-NTA biosensors (FortéBio) were preequilibrated in buffer before coating with C-terminal hexahistidine MALT1 (339–719) at 375 nM for 600 s. MALT1 was titrated with increasing concentrations (0.0, 0.01, 0.025, 0.05, 0.2, 0.5, 0.8, and 1.2 mM) of untagged ubiquitin (Sigma-Aldrich, U6253) for a total time of 180 s association followed by a 300 s dissociation step. Experiments described above were run for the following ligand–analyte couples: MALT1 WT-ubiquitin WT, MALT1 WT-ubiquitin K6A, MALT1 WT-ubiquitin K48A, and MALT1 WT-ubiquitin H68A. Raw data were corrected by double referencing and analyzed using Prism7 software (GraphPad).

Statistical Analysis. Parametric two-tailed Student's *t* test or one-way ANOVA with Dunnett correction were used for statistical analysis; P values ≤ 0.05 were considered statistically significant.

Data Availability Statement. All data supporting the findings of this paper are available upon request from the corresponding authors (M.T. and M.D.C.).

ACKNOWLEDGMENTS. The authors thank the Protein Modeling Facility of the University of Lausanne for support with structural modeling, Nagham Alouche and Daniela Chmiest for help with setting up primary T cell experiments, Mélanie Juilland-Favre for help with artwork, and Fabio Martinon for comments on the paper. This work was supported by grants (to M.T.) from the Swiss National Science Foundation (310030_166627), the Swiss Cancer League (KFS-4095-02-2017), and the Emma Muschamp Foundation. Structural and biophysical studies at Leicester were supported by a research partnership with LifeArc. The NMR facilities at Leicester were supported by grants from the Wellcome Trust and EPSRC.

1. J. Ruland, G. S. Duncan, A. Wakeham, T. W. Mak, Differential requirement for Malt1 in T and B cell antigen receptor signaling. *Immunity* **19**, 749–758 (2003).
2. A. A. Ruefli-Brasse, D. M. French, V. M. Dixit, Regulation of NF-kappaB-dependent lymphocyte activation and development by paracaspase. *Science* **302**, 1581–1584 (2003).
3. M. Jaworski *et al*., Malt1 protease inactivation efficiently dampens immune responses but causes spontaneous autoimmunity. *EMBO J.* **33**, 2765–2781 (2014).
4. A. Gewies *et al*., Uncoupling Malt1 threshold function from paracaspase activity results in destructive autoimmune inflammation. *Cell Rep.* **9**, 1292–1305 (2014).
5. J. W. Yu *et al*., MALT1 protease activity is required for innate and adaptive immune responses. *PLoS One* **10**, e0127083 (2015).
6. F. Bornancin *et al*., Deficiency of MALT1 paracaspase activity results in unbalanced regulatory and effector T and B cell responses leading to multiorgan inflammation. *J. Immunol.* **194**, 3723–3734 (2015).
7. S. Rosebeck, A. O. Rehman, P. C. Lucas, L. M. McAllister-Lucas, From MALT lymphoma to the CBM signalosome: Three decades of discovery. *Cell Cycle* **10**, 2485–2496 (2011).

8. J. Ruland, L. Hartjes, CARD-BCL-10-MALT1 signalling in protective and pathological immunity. *Nat. Rev. Immunol.* **19**, 118–134 (2019).
9. F. Schlauderer *et al*., Molecular architecture and regulation of BCL10-MALT1 filaments. *Nat. Commun.* **9**, 4041 (2018).
10. Q. Qiao *et al*., Structural architecture of the CARMA1/Bcl10/MALT1 signalosome: Nucleation-induced filamentous assembly. *Mol. Cell* **51**, 766–779 (2013).
11. A. G. Uren *et al*., Identification of paracaspases and metacaspases: Two ancient families of caspase-like proteins, one of which plays a key role in MALT lymphoma. *Mol. Cell* **6**, 961–967 (2000).
12. H. Zhou, M. Q. Du, V. M. Dixit, Constitutive NF-kappaB activation by the t(11;18)(q21;q21) product in MALT lymphoma is linked to deregulated ubiquitin ligase activity. *Cancer Cell* **7**, 425–431 (2005).
13. C. Wiesmann *et al*., Structural determinants of MALT1 protease activity. *J. Mol. Biol.* **419**, 4–21 (2012).
14. J. W. Yu, P. D. Jeffrey, J. Y. Ha, X. Yang, Y. Shi, Crystal structure of the mucosa-associated lymphoid tissue lymphoma translocation 1 (MALT1) paracaspase region. *Proc. Natl. Acad. Sci. U.S.A.* **108**, 21004–21009 (2011).
15. C. Pelzer *et al*., MALT1 protease activity is controlled by monoubiquitination. *Nat. Immunol.* **14**, 337–345 (2013).
16. G. Lenz *et al*., Oncogenic CARD11 mutations in human diffuse large B cell lymphoma. *Science* **319**, 1676–1679 (2008).
17. S. Hailfinger *et al*., Malt1-dependent RelB cleavage promotes canonical NF-kappaB activation in lymphocytes and lymphoma cell lines. *Proc. Natl. Acad. Sci. U.S.A.* **108**, 14596–14601 (2011).
18. J. Staal *et al*., T-cell receptor-induced JNK activation requires proteolytic inactivation of CYLD by MALT1. *EMBO J.* **30**, 1742–1752 (2011).
19. S. Polo *et al*., A single motif responsible for ubiquitin recognition and monoubiquitination in endocytic proteins. *Nature* **416**, 451–455 (2002).
20. D. Hoeller *et al*., E3-independent monoubiquitination of ubiquitin-binding proteins. *Mol. Cell* **26**, 891–898 (2007).
21. M. Düwel *et al*., A20 negatively regulates T cell receptor signaling to NF-kappaB by cleaving Malt1 ubiquitin chains. *J. Immunol.* **182**, 7718–7728 (2009).
22. L. Sun, L. Deng, C. K. Ea, Z. P. Xia, Z. J. Chen, The TRAF6 ubiquitin ligase and TAK1 kinase mediate IKK activation by BCL10 and MALT1 in T lymphocytes. *Mol. Cell* **14**, 289–301 (2004).
23. H. Noels *et al*., A novel TRAF6 binding site in MALT1 defines distinct mechanisms of NF-kappaB activation by API2middle dotMALT1 fusions. *J. Biol. Chem.* **282**, 10180–10189 (2007).
24. L. Deng *et al*., Activation of the IkappaB kinase complex by TRAF6 requires a dimeric ubiquitin-conjugating enzyme complex and a unique polyubiquitin chain. *Cell* **103**, 351–361 (2000).
25. F. Rebeaud *et al*., The proteolytic activity of the paracaspase MALT1 is key in T cell activation. *Nat. Immunol.* **9**, 272–281 (2008).
26. J. Hachmann *et al*., Mechanism and specificity of the human paracaspase MALT1. *Biochem. J.* **443**, 287–295 (2012).
27. I. Dikic, S. Wakatsuki, K. J. Walters, Ubiquitin-binding domains–from structures to functions. *Nat. Rev. Mol. Cell Biol.* **10**, 659–671 (2009).
28. K. Cabalzar *et al*., Monoubiquitination and activity of the paracaspase MALT1 requires glutamate 549 in the dimerization interface. *PLoS One* **8**, e72051 (2013).
29. D. Nagel *et al*., Pharmacologic inhibition of MALT1 protease by phenothiazines as a therapeutic approach for the treatment of aggressive ABC-DLBCL. *Cancer Cell* **22**, 825–837 (2012).
30. L. Fontan *et al*., MALT1 small molecule inhibitors specifically suppress ABC-DLBCL in vitro and in vivo. *Cancer Cell* **22**, 812–824 (2012).
31. C. Mc Guire *et al*., Pharmacological inhibition of MALT1 protease activity protects mice in a mouse model of multiple sclerosis. *J. Neuroinflammation* **11**, 124 (2014).
32. M. Di Pilato *et al*., Targeting the CBM complex causes T_{reg} cells to prime tumours for immune checkpoint therapy. *Nature* **570**, 112–116 (2019).
33. M. Rosenbaum *et al*., Bcl10-controlled Malt1 paracaspase activity is key for the immune suppressive function of regulatory T cells. *Nat. Commun.* **10**, 2352 (2019).
34. L. Cheng, N. Deng, N. Yang, X. Zhao, X. Lin, Malt1 protease is critical in maintaining function of regulatory T cells and may be a therapeutic target for antitumor immunity. *J. Immunol.* **202**, 3008–3019 (2019).
35. S. M. Lim *et al*., Identification of β-lapachone analogs as novel MALT1 inhibitors to treat an aggressive subtype of diffuse large B-cell lymphoma. *J. Med. Chem.* **58**, 8491–8502 (2015).
36. B. T. Xin *et al*., Development of new Malt1 inhibitors and probes. *Bioorg. Med. Chem.* **24**, 3312–3329 (2016).
37. J. Quancard *et al*., An allosteric MALT1 inhibitor is a molecular corrector rescuing function in an immunodeficient patient. *Nat. Chem. Biol.* **15**, 304–313 (2019).
38. A. Schlapbach *et al*., N-aryl-piperidine-4-carboxamides as a novel class of potent inhibitors of MALT1 proteolytic activity. *Bioorg. Med. Chem. Lett.* **28**, 2153–2158 (2018).
39. D. Rueda *et al*., Bcl10 controls TCR- and FcgammaR-induced actin polymerization. *J. Immunol.* **178**, 4373–4384 (2007).